Synthesis and Pharmacology of N^1-Substituted Piperazine-2,3-dicarboxylic Acid Derivatives Acting as NMDA Receptor Antagonists

Richard M. Morley,[†] Heong-Wai Tse,[†] Bihua Feng,[‡] Jacqueline C. Miller,[†] Daniel T. Monaghan,[‡] and David E. Jane*,[†]

Department of Pharmacology, MRC Centre for Synaptic Plasticity, School of Medical Sciences, University Walk, University of Bristol, Bristol, BS8 1TD, UK, and Department of Pharmacology, University of Nebraska Medical Center, Omaha, Nebraska 68198-6260

Received September 15, 2004

The binding site for competitive NMDA receptor antagonists is on the NR2 subunit, of which there are four types (NR2A−D). Typical antagonists such as (*R*)-AP5 have a subunit selectivity of NR2A > NR2B > NR2C > NR2D. The competitive NMDA receptor antagonist (2*R**,3*S**)-(1-biphenylyl-4-carbonyl)piperazine-2,3-dicarboxylic acid (PBPD, **16b**) displays an unusual selectivity with improved relative affinity for NR2C and NR2D vs NR2A and NR2B. Analogues of **16b** bearing aroyl or aryl substituents attached to the N^1 position of piperazine-2,3-dicarboxylic acid have been synthesized to probe the structural requirements for NR2C/NR2D selectivity. A phenanthrenyl-2-carbonyl analogue, **16e**, had >60-fold higher affinity for NR2C and NR2D and showed 3−5-fold selectivity for NR2C/NR2D vs NR2A/NR2B. The phenanthrenyl-3-carbonyl analogue (**16f**) was less potent but more selective, having 5- and 7-fold selectivity for NR2D vs NR2A and NR2B, respectively. Thus, antagonists bearing bulky hydrophobic residues have a different NR2 subunit selectivity than that of typical antagonists.

Introduction

Ionotropic glutamate receptors are glutamate-gated ion channels that have been classified into three main types, the *N*-methyl-D-aspartate (NMDA, **1**, Figure 1), AMPA, and kainate receptors based on their pharmacology and more recently their amino acid sequence homology.[1,2] The NMDA receptors play an important role in synaptic transmission and in particular in neuronal synaptic plasticity, which is thought to underlie learning and memory. In addition, NMDA receptors are involved in a variety of pathological conditions, including epilepsy, pain-related disorders, and disorders arising from neuronal cell death following stroke or head injury as well as psychiatric disorders such as schizophrenia.[3]

NMDA receptors are composed of subunits from the NR1a−h and NR2A−D families of subunits. The NR3A subunit may play a regulatory role in the functioning of some NMDA receptors likely controlling Ca^{2+} ion influx through the channel.[4] The glutamate recognition site is located on the NR2 subunit,[5] while the glycine coagonist binding site is located on the NR1 subunit.[6] It has been proposed that the different NR2 subunits may be responsible for the distinct glutamate binding site pharmacologies of NR1/NR2 combinations[7−9] and that this may underlie the diverse NMDA receptor pharmacologies in native rat brain regions.[8,10,11] The first potent and selective antagonists, such as (*R*)-AP5 (**2**) and (*R*)-AP7 (**3**) described by Watkins and coworkers[12] and those described later based on the structure of these lead compounds (such as CPP, **4**),[13] had very similar patterns of selectivity when tested on native or recombinant NMDA receptors[8,14,15] (see Figure 1 for structures). In general, the rank order of potency of the competitive antagonists that have been tested on recombinant NMDA receptors is NR2A > NR2B > NR2C > NR2D. The only subunit selective antagonists are selective for the polyamine binding site(s) on the NR2B subunit, which is distinct from the glutamate binding site.[2] Recently, a competitive antagonist based on the quinoxalinedione nucleus, PEAQX (**5**, Figure 1), has been reported to be selective for NR2A vs NR2B;[16] however, this compound has little selectivity for NR2A vs NR2C or NR2D.[17] In our search for subunit selective NMDA receptor antagonists we have identified PBPD (**16b**, Figure 1), which has an unusual selectivity profile, NR2D > NR2B > NR2C > NR2A.[9] We have hypothesized that the moderately potent antagonist activity exhibited by **16b** is probably due to the interaction of the hydrophobic biphenyl residue with hydrophobic amino acid residues within the receptor and that this interaction may be responsible for the unique NR2 subunit selectivity of **16b**. We report herein the syn-

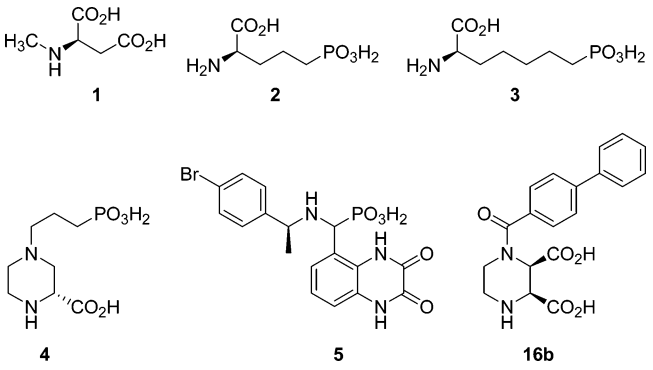

Figure 1. Structures of NMDA and previously reported competitive NMDA receptor antagonists.

* To whom correspondence should be addressed. Phone: +44 (0)117 9546451. Fax: +44 (0)117 9250168. E-mail: david.jane@bristol.ac.uk.
[†] University of Bristol.
[‡] University of Nebraska Medical Center.

10.1021/jm0492498 CCC: $30.25
Published on Web 02/18/2005

Scheme 1[a]

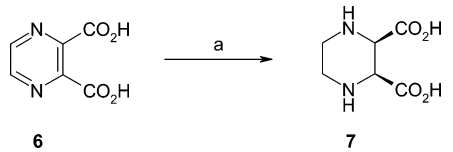

[a] Reagents and conditions: (a) (i) KOH (aq), 10% Pd/C, H_2, (ii) HNO_3, (iii) DOWEX 50WX8-400 H^+ form ion-exchange resin.

Scheme 2[a]

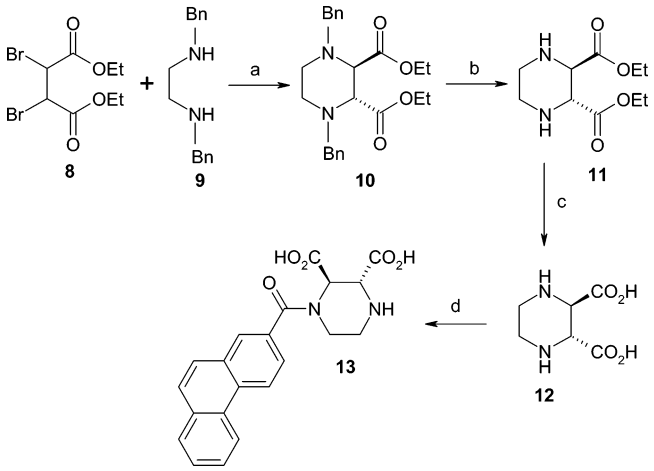

[a] Reagents and conditions: (a) Et_3N, C_6H_6; (b) 10% Pd/C, H_2, EtOH; (c) (i) NaOH, EtOH (ii) HNO_3 (aq), (iii) DOWEX 50WX8-400 H^+ form ion-exchange resin.

thesis of **16b** and a range of new analogues with the aim of probing the hydrophobic binding site and investigating how modification of the hydrophobic substituent influences NR2 subunit selectivity. The compounds have been evaluated as antagonists of currents coactivated by (*S*)-glutamate and glycine in *Xenopus* oocytes expressing rat recombinant NR1a/NR2 subunits.

Results

Chemistry. The starting material for most of the compounds synthesized was the meso-isomer (2*R**,3*S**)-piperazine-2,3-dicarboxylic acid (**7**). This could conveniently be prepared in good yield by palladium-catalyzed hydrogenation of the corresponding pyrazine (**6**) (Scheme 1). It has been previously reported that this method gives the (2*R**,3*R**)-isomer (**12**), as the product could be resolved to give the two enantiomers.[18] It is possible that previous workers detected a small rotation ($[\alpha]_D = +$ or $-$ 0.3) in their "resolved product" due to contamination from the trans-isomer, which may have been produced via epimerization during the course of the resolution procedure. In support of this theory, the rotation values for the separate enantiomers were obtained from a solution of 20 g/100 mL, and therefore, even a low percentage contamination of the resolved trans-isomer would be enough to give a small rotation. To determine whether hydrogenation of **6** led to the cis- or trans-isomer, an independent synthesis of **12** was undertaken. A method reported to give **12** in good yield[19] involving reaction of **8**[20] (Scheme 2) with *N*,*N*-bis-*p*-tolylsulfonylethylene-1,2-diamine was attempted, but in our hands this method gave only poor yields of the required compound and suffered from the disadvantage of having to remove the *p*-tolylsulfonamide groups, which proved difficult. A modification of this method in which the benzyl protected diamine (**9**) was reacted with **8** gave the protected piperazine (**10**) in reasonable yield. This gave the required (2*R**,3*R**)-isomer (**2**) upon catalytic hydrogenation to remove the benzyl protecting groups and hydrolysis of the resulting ester (**11**) in ethanolic sodium hydroxide. Compound **10** proved to have the trans-(2*R**,3*R**)-configuration when analyzed using X-ray crystallography (Figure 2) and by implication **12** must have the (2*R**,3*R**)-configuration. The ^{1}H NMR spectra of **12** and **7** were found to be different and therefore the isomer produced by catalytic hydrogenation of **6** must have the cis-(2*R**,3*S**)-configuration.

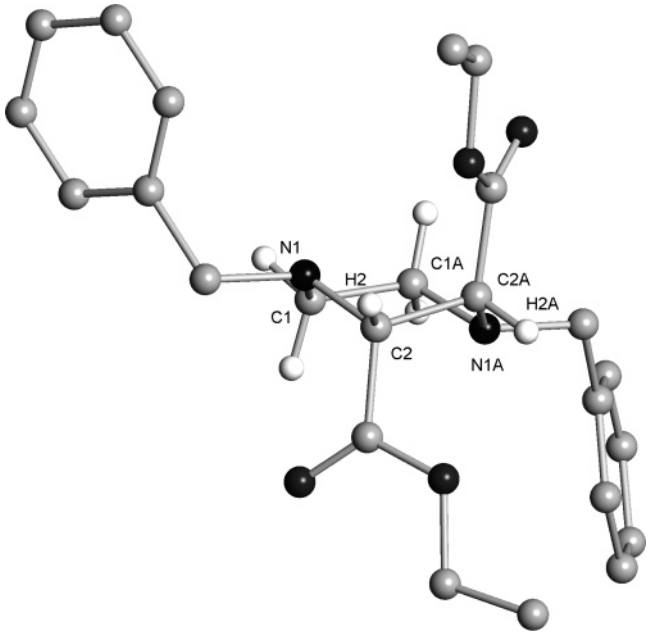

Figure 2. Molecular structure of **10** illustrating the trans arrangement of the ethyl carboxylate groups. Ethyl and benzyl hydrogen atoms have been omitted for clarity.

A series of *N*-substituted analogues (**16a**−**n**) of **7** including the lead compound **16b** were prepared using modified Schotten−Baumen conditions by reacting the acid chlorides (**15a**−**n**) with the cis-(2*R**,3*S**)-isomer **7** in the presence of sodium hydroxide in aqueous dioxane (Scheme 3). The acid chlorides (**15a**−**n**) were prepared from the corresponding carboxylic acids (**14a**−**n**) by treatment with excess thionyl chloride. The carboxylic acids (**14a**−**n**) were either commercially available or were synthesized by standard methods. The final products (**16a**−**n**) were conveniently isolated by acidification of the reaction mixture and could be readily purified by redissolving in aqueous sodium hydroxide, acidification with hydrochloric acid, and washing the resulting precipitate with dioxane to remove contaminating carboxylic acid starting material. Crystallization from hot water was avoided, as this led to hydrolysis of the amide back to the carboxylic acid. The low yield (10−30%) observed for a number of the products is likely due to hydrolysis of the acid chloride in the aqueous basic conditions and possibly also due to formation of N^1,N^4-disubstituted compounds that were not isolated using the workup conditions described. The ^{1}H NMR spectra of **16a**−**n** have two sets of doublets for the methine protons on the piperazine ring, suggesting that two rotamers are present on the NMR time scale due to restricted rotation around the amide bond.

Scheme 3[a]

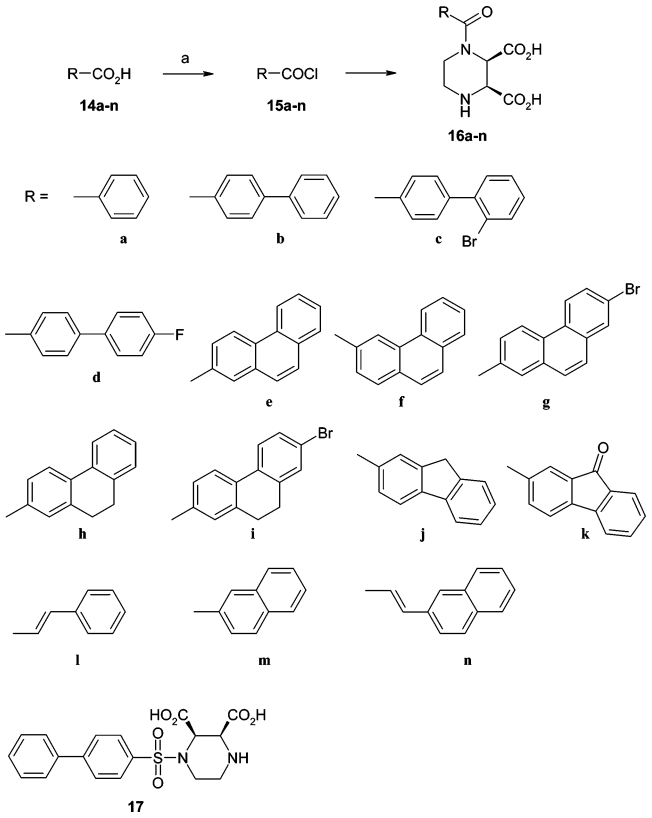

[a] Reagents and conditions: (a) $SOCl_2$, C_6H_6, 80 °C, 12 h; (b) (i) **7**, NaOH, dioxane/H_2O (2:1), 0 °C, 2 h and then rt, 12 h, (ii) 2 M HCl (aq).

To investigate the role of the amide group on NMDA receptor antagonist activity, compounds were synthesized that had a sulfonyl (**17**, Scheme 3) or a methylene (**23**) rather than a carbonyl group between the N^1 atom of **7** and the aryl moiety. The sulfonyl derivative (**17**) was synthesized under similar conditions to those used for the synthesis of **16a**−**n** by reacting commercially available biphenylsulfonyl choride with **7**. The methylene derivative (**23**) was synthesized by alkylation of **21** with the iodomethylphenanthrene (**19**) and hydrolysis of the intermediate (**22**) with lithium hydroxide in THF/H_2O. The synthesis of **19** was achieved by reduction of carboxylic acid (**14e**) with lithium aluminum hydride and treatment of the resulting alcohol (**18**)[21] with potassium iodide and boron trifluoride etherate in dioxane (Scheme 4).[22] The piperazine (**21**) was obtained by palladium-catalyzed hydrogenation of pyrazine (**20**). The coupling constants for the methine protons on the piperazine ring of **23** were very similar to those for the cis-isomer **16e** and larger than those for the trans-isomer **13**, suggesting that the carboxylic acid groups have the cis-configuration in compound **23**. There was no evidence for the presence of rotamers in the ^1H NMR spectrum of **23**, backing up the theory that the presence of two sets of doublets for the methine protons on the carbon atom α to the carboxylic acid groups on the piperazine ring in **16a**−**n** is due to rotamers caused by restricted rotation around the amide bond.

To determine whether a cis or trans arrangement of the carboxylic acid groups on the piperazine ring was necessary for activity at NMDA receptors, the trans-(2*R**,3*R**)-isomer (**13**) was synthesized. The synthesis

Scheme 4[a]

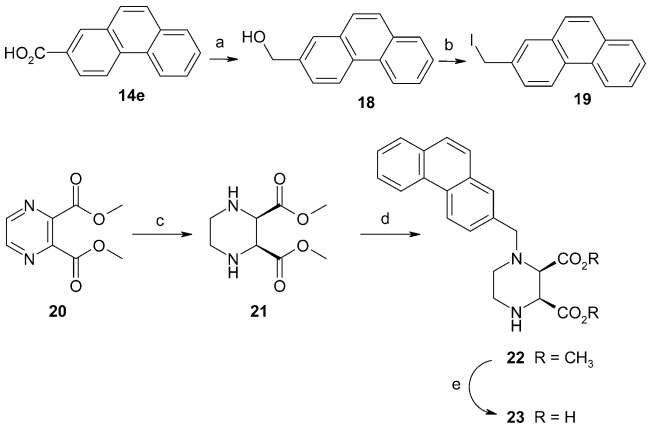

[a] Reagents and conditions: (a) (i) $LiAlH_4$, THF, (ii) NH_4Cl (aq); (b) KI, $BF_3{\cdot}Et_2O$, dioxane; (c) H_2 10% Pd/C; (d) (i) **20**, Et_3N, THF, 0 °C, 2 h and then room temp, 12 h; (e) (i) LiOH, THF/H_2O (2:1), (ii) 2 M HCl (aq).

of **13** was accomplished by acylation of **12** with acid chloride (**15e**) under modified Schotten−Baumen conditions.

Pharmacology. Activity at Recombinant NMDA Receptors. The antagonist effects of compounds were tested on each of the four different NR2 subunits coexpressed with NR1a in *Xenopus* oocytes using an electrophysiological assay. Variations in NR1 subunits splice forms were not examined because they do not have the glutamate binding site and because there is no evidence that the splice forms alter glutamate-site antagonist specificity. Each of the four NR2 subunits was examined, since these represent the four genetically distinct glutamate binding sites.[8,10,11] These four binding sites account for essentially all of the known variations in glutamate-site antagonist specificity at the NMDA receptors from both physiological and radioligand binding experiments.[8,9,14,15] Antagonist activity was measured as IC_{50} values for the depression of currents evoked by stimulation with (*S*)-glutamate (10 μM) and glycine (10 μM). These IC_{50} values were converted to K_i values to take into account differences in agonist potency for the different NR2 subunits.

The K_i values of all of the new compounds and four reference substances (**2**−**5**) are presented in Table 1, while Table 2 contains the data normalized to the K_i values for NR2C to gain a better appreciation of the NR2 subunit selectivity of the compounds. Unlike the reference substances **2**−**4**, which display a rank order of potency of NR2A> NR2B > NR2C > NR2D, **16b** displayed an unusual subunit selectivity with the rank order of potency being NR2D > NR2B > NR2C > NR2A though the difference in K_i values was only 3-fold at the most. An analogue of **16b** with only one benzene ring attached to the carbonyl group (**16a**) was inactive at all NR2 subunits up to a concentration of 100 μM. The 2′-bromobiphenylyl-substituted derivative (**16c**) had approximately the same affinity for NR2C but much lower affinity for the other NR2 subunits than **16b** and displayed selectivity for NR2C. In contrast, the 4′-fluorobiphenylyl-substituted derivative (**16d**) had approximately 2-fold greater affinity for NR2A compared to **16b** and as a result had less than a 2-fold difference in affinity across all four NR2 subunits. When the first aromatic ring of **16b** was replaced with an (*E*)-ethenyl

Table 1. Antagonist K_i Values (μM) for Inhibiting the Responses of Recombinant Rat NMDA Receptors Expressed in *Xenopus* Oocytes (means ± SEM (*n*))

	NR1a/NR2A	NR1a/NR2B	NR1a/NR2C	NR1a/NR2D
2, (*R*)-AP5[a]	0.28 ± 0.02	0.46 ± 0.14	1.64 ± 0.14	3.71 ± 0.67
3, (*R*)-AP7	0.49 ± 0.18 (5)	4.14 ± 0.36 (5)	6.42 ± 1.08 (6)	17.10 ± 0.65 (5)
4, (*R*)-CPP	0.041 ± 0.003 (6)	0.27 ± 0.02 (5)	0.63 ± 0.05 (5)	1.99 ± 0.20 (5)
5, PEAQX	0.0054 ± 0.0004 (5)	0.067 ± 0.003 (5)	0.0116 ± 0.0009 (5)	0.037 ± 0.004 (4)
16a, UBP130	>100	>100	>100	>100
16b, PBPD[a]	15.79 ± 0.43	5.01 ± 0.25	8.98 ± 0.18	4.29 ± 0.11
16c, UBP101	42.9 ± 5.3 (4)	22.1 ± 5.2 (5)	8.49 ± 0.72 (4)	12.9 ± 1.1 (4)
16d, UBP102	8.78 ± 0.88 (5)	13.4 ± 0.8 (5)	7.38 ± 0.38 (5)	8.02 ± 0.31 (5)
16e, PPDA	0.55 ± 0.15 (3)	0.31 ± 0.02 (5)	0.096 ± 0.006 (4)	0.125 ± 0.035 (5)
16f, UBP141	14.19 ± 1.11 (5)	19.29 ± 1.38 (4)	4.22 ± 0.52 (6)	2.78 ± 0.16 (5)
16g, UBP142	0.3200 ± 0.0164 (5)	0.2500 ± 0.0268 (5)	0.0994 ± 0.0043 (5)	0.1500 ± 0.0095 (5)
16h, UBP135	1.54 ± 0.11 (6)	0.76 ± 0.11 (5)	0.29 ± 0.02 (5)	0.57 ± 0.03 (5)
16i, UBP137	3.88 ± 0.19 (5)	2.15 ± 0.31 (5)	0.66 ± 0.07 (4)	1.03 ± 0.09 (5)
16j, UBP132	4.43 ± 0.44 (6)	3.25 ± 0.21 (6)	1.17 ± 0.06 (5)	2.17 ± 0.32 (6)
16k, UBP106	7.97 ± 0.77 (4)	9.36 ± 1.41 (6)	4.42 ± 0.40 (6)	6.45 ± 0.40 (5)
16l, UBP112	13.2 ± 0.89 (5)	18.0 ± 2.4 (4)	27.0 ± 3.1 (5)	59.7 ± 8.5 (6)
16m, UBP131	9.6 ± 1.1 (5)	18.2 ± 1.3 (5)	3.89 ± 0.09 (5)	9.26 ± 0.43 (6)
16n, UBP129	0.84 ± 0.08 (10)	0.3 ± 0.06 (4)	0.85 ± 0.19 (5)	1.94 ± 0.14 (5)
17, UBP124	13.6 ± 1.8 (5)	16.2 ± 4.1 (5)	8.67 ± 0.62 (5)	10.88 ± 0.45 (5)
23, UBP140	11.18 ± 1.29 (4)	10.25 ± 1.87 (4)	2.67 ± 0.13 (4)	3.18 ± 0.19 (4)
13, UBP138	10.48 ± 1.23 (5)	9.08 ± 1.02 (3)	4.88 ± 0.57 (5)	6.03 ± 2.01 (3)

[a] Values for **2** and **16b** represent $n = 4-6$ from ref 9.

Table 2. Potency Relative to Activity on NR1a/NR2C (K_i NR2/K_i NR2C)

	NR1a/NR2A	NR1a/NR2B	NR1a/NR2D
2, (*R*)-AP5	0.17	0.28	2.26
3, (*R*)-AP7	0.076	0.64	2.66
4, (*R*)-CPP	0.065	0.43	3.16
5, PEAQX	0.47	5.78	3.19
16b, PBPD	1.76	0.56	0.48
16c, UBP101	5.05	2.6	1.52
16d, UBP102	1.19	1.81	1.09
16e, PPDA	5.73	3.23	1.3
16f, UBP141	3.36	4.57	0.66
16g, UBP142	3.2	2.5	1.51
16h, UBP135	5.3	2.62	1.97
16i, UBP137	5.88	3.26	1.56
16j, UBP132	3.79	2.78	1.85
16k, UBP106	1.8	2.12	1.46
16l, UBP112	0.49	0.66	2.2
16m, UBP131	2.47	4.68	2.38
16n, UBP129	0.99	0.35	2.28
17, UBP124	1.57	1.87	1.25
23, UBP140	4.19	3.84	1.19
13, UBP138	2.15	1.86	1.24

linker to give **16l**, there was a 3−10-fold loss of affinity across the NR2B−D subunits but a slight increase in affinity on NR2A. Compound **16l** therefore had a NR2 subunit selectivity similar to typical competitive antagonists such as **2**. When the carbonyl group linking the biphenyl ring of **16b** to the piperazine ring was replaced with a sulfonyl linker to give **17**, there was a decrease in affinity for NR2B and NR2D which resulted in the NR2 selectivity of **17** being less than 2-fold across the four NR2 subunits.

A dramatic increase in potency was observed when the two phenyl rings of **16b** were joined together by an additional phenyl ring, thereby making the aromatic rings coplanar. The resulting compound **16e** had much higher affinity across all of the NR2 subunits than the parent compound **16b** with K_i values of 96 ± 6 and 125 ± 35 nM on NR2C and NR2D (an ANOVA with Newman−Keuls multiple comparison test suggests that the K_i values for the NR2 subunits were significantly different from each other except between NR2C and NR2D). In addition, **16e** showed selectivity for NR2C and NR2D vs NR2A and NR2B, which is the opposite of "typical" competitive NMDA receptor antagonists such as **2**. A positional isomer of **16e** with the carbonyl linker attached to the 3-position of the phenanthrene ring (**16f**) had lower affinity across all of the NR2 subunits but showed a 5- and 7-fold selectivity for NR2D vs NR2A and NR2B, respectively. The 7-bromo analogue **16g** of **16e** had marginally less affinity than **16e** for NR2C and NR2D but had slightly higher affinity for NR2A and NR2B and was therefore less selective for NR2C/NR2D overall. A saturated ethylene bridge between the two phenyl rings was not as well tolerated, as **16h** had lower affinity than **16e** across all four NR2B subunits, though it did show a similar pattern of NR2 subunit selectivity to **16e**. The 7-bromo analogue **16i** had ∼2-fold lower affinity across the NR2 subunits than **16h** but showed almost 6-fold selectivity for NR2C vs NR2A, making it the most NR2C selective antagonist tested. Replacement of the ethylene bridge with either a methylene (**16j**) or keto (**16k**) group spacer resulted in a much decreased affinity across all NR2 subunits compared to **16e** and also a decrease in the NR2C/NR2D vs NR2A/NR2B selectivity. Compound **16m** in which the last aromatic ring of **16e** is missing had much lower affinity for NR2C and NR2D than **16e** but showed almost 5-fold selectivity for NR2C vs NR2B. In agreement with the observed AP5-like pattern of activity of **16l**, an analogue of **16e** with an ethenyl linker instead of the first phenyl ring **16n** had higher affinity for NR2B than NR2C and NR2D but unlike **2** had similar affinity for NR2A and NR2C.

Replacement of the carbonyl linker in **16e** with a methylene group to give compound **23** resulted in a 20−30-fold lowering of affinity across all four subunits, but the pattern of NR2 subunit selectivity was similar to that of **16e**. Changing from a cis- to a trans-configuration of the carboxylic acid groups on the piperazine ring of **16e** also resulted in a lowering of affinity across all four subunits. In this case compound **13** had an ∼50-fold lower affinity on NR2C and NR2D compared to **16e** and a lower selectivity for NR2C vs NR2A and NR2B.

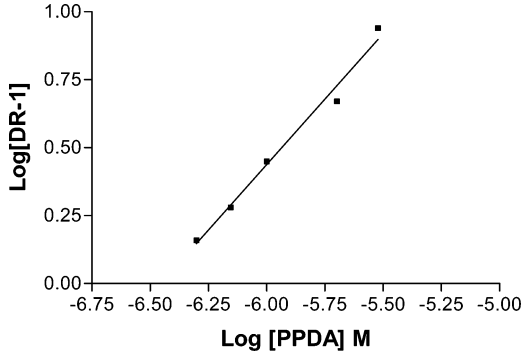

Figure 3. Schild analysis of the antagonism of NMDA-induced depolarizations of neonatal rat motoneurones by five different concentrations of **16e**. Each point represents the mean of three independent determinations of the dose ratio (DR).

Activity at NMDA Receptors on Neonatal Rat Spinal Motoneurones. The most potent antagonist identified in this study **16e** was tested as an antagonist of NMDA-induced depolarizations of neonatal rat motoneurones. To calculate the pA_2 value for the antagonism of NMDA-induced depolarizations by **16e**, noncumulative concentration−response curves for NMDA were constructed both in the absence and presence of 0.5, 0.7, 1, 2, and 3 μM **16e**. From a Schild plot of the data (Figure 3) a pA_2 value of 6.45 and a slope of 0.96 ± 0.07 ($n = 3$ for each data point) was calculated suggestive of a competitive mode of antagonism.

Discussion

Most of the competitive NMDA receptor antagonists reported to date are conformationally restricted analogues based on the structure of **2** or **3**.[23,24] These antagonists tend to display a typical pattern of selectivity on recombinant NR2 subunits with the rank order of affinity being NR2A > NR2B > NR2C > NR2D.[8,14,15] We have previously evaluated the four reference substances in Table 1 including the well-established antagonists **2**, **3**, and **4**[12,13] and the recently reported NR2A-selective antagonist **5**[16] as antagonists of recombinant NMDA receptors. Three of the reference substances (**2**−**4**) used in this study displayed the "typical" competitive antagonist profile noted for antagonists based on the AP5 or AP7 structure. Indeed, **4** displayed the greatest selectivity for NR2A vs NR2D, with approximately 50-fold higher affinity for NR2A than NR2D. However, **5** displayed a higher affinity for NR2A- and NR2C-containing receptors than for NR2B- and NR2D-containing receptors, but in our hands it did not display the >100-fold difference in affinity between NR2A and NR2B reported by Auberson et al.[16] This may be due to a species difference, as rat rather than human recombinant NMDA receptors were used in the present study.

We have previously reported that a few competitive NMDA receptor antagonists display an altered pattern of NR2 subunit selectivity. The conformationally restricted AP7 analogue (3*S*,4a*R*,6*S*,8a*R*)-6-(1*H*-tetrazol-5-ylmethyl)decahydroisoquinoline-3-carboxylic acid (LY233536) and the AP5 analogue with a bulky biphenyl-containing substituent (*S*)-2-amino-3-(5-phosphonomethylbiphenyl-3-yl)propionic acid (EAB-515) display a higher affinity for NR2B than for NR2A-containing receptors and have an improved relative affinity for NR2C- and NR2D-containing receptors.[9] Thus, bulky hydrophobic substituents alter the subunit specificity of NMDA receptor antagonists. It has been proposed that the biphenyl group of EAB-515 binds to a hydrophobic binding pocket[25,26] presumably corresponding to the "allowed" region described in antagonist modeling studies.[23]

A conformationally restricted analogue (**16b**) of **1** has been previously shown to be an NMDA receptor antagonist.[9] Normally competitive NMDA receptor antagonists have five or seven bonds between the proximal and distal acidic groups. Unusually, although **16b** is an antagonist, it has a short interacidic group chain length that is more commonly observed with agonists such as **1**.[23] It is therefore likely that the amino acid end of **16b** is binding to the same sites in the receptor as **1** and that it is the large bulky biphenyl ring substituent that is responsible for the antagonist activity. We have shown that **16b** displays a higher affinity for NR2B than for NR2A and has an improved relative affinity for NR2C- and NR2D-containing vs NR2A- and NR2B-containing receptors, and it is likely that the bulky biphenyl residue is responsible for this unusual NR2 subunit selectivity.[9]

Though the difference in affinity between NR2D and NR2A was only 3-fold, **16b** represents a lead for the development of NR2D selective antagonists. A series of compounds based on the structure of **16b** was designed to investigate the effect on NR2 subunit selectivity of adding substituents to the aryl ring (**16c**,**d**,**g**,**i**), the position of substitution of the carbonyl linker on the aromatic ring (**16f**), changing the aromatic ring (**16a**, **e**,**h**,**j**−**n**), the nature of the group linking the aryl ring to the piperazine ring (**17** and **23**), and the configuration of the carboxylic acid groups attached to the piperazine ring (**16e** and **13**).

In general, structural modifications of **16b** did not lead to antagonists with high selectivity for individual NR2 subunits (see Tables 1 and 2). However, some of the structural alterations did change the affinity for certain NR2 subunits and also changed the pattern of NR2 subunit selectivity observed with **16b**. The most profound effect was observed upon substituting the biphenyl ring of **16b** with a phenanthrene ring to form **16e**. This has the effect of locking the first and last aromatic rings of the biphenyl substituent into a coplanar arrangement, which is different than that observed with the biphenyl ring system, where the benzene rings are twisted out of the plane. The effect on the affinity across all four NR2 subunits was dramatic as **16e** had 94- and 64-fold higher affinity for NR2C and NR2D, respectively, while increases in affinity on NR2A and NR2B were more modest. The pattern of selectivity was NR2C > NR2D > NR2B > NR2A and **16e** was almost 6-fold selective for NR2C vs NR2A.

It has been previously reported that the N^1-4-bromobenzoyl and N^1-4-chlorobenzoyl analogues of *cis*-piperazine-2,3-dicarboxylic acid are selective for NMDA vs non-NMDA receptors in the hippocampus, but the selectivity is reversed when these compounds were tested on neonatal rat spinal cord motoneurones.[27,28]

The activity of these compounds on non-NMDA receptors was fairly weak (K_D values > 500 μM). Preliminary data from binding studies suggests that **16e** has about 100-fold higher affinity at NMDA vs AMPA receptor binding sites (D.T.M., unpublished observations).

A positional isomer of **16e** with the carbonyl linker attached to the 3-position of the phenanthrene ring (**16f**) had 40- and 20-fold lower affinity for NR2C and NR2D, respectively; however, this compound had a similar pattern of selectivity to **16e**. Indeed **16f** was more selective than **16e**, being 5- and 7-fold selective for NR2D vs NR2A and NR2B, respectively making it the most selective NR2D antagonist reported to date. Thus, the position of substitution of the carbonyl linker on the aromatic moiety has a profound effect on the affinity for each of the NR2 subunits and also influences NR2D selectivity.

Substituting the phenanthrene ring of **16e** for a 9,10-dihydrophenanthrene ring to form **16h** resulted in a 3−5-fold reduction of affinity for NR2C and NR2D and also lowered NR2C selectivity, suggesting that a coplanar arrangement of the aromatic rings is favored for binding to NR2C and NR2D. An additional consideration is that the π electrons in the middle ring may be contributing to the interaction between the ligand and the receptor. If either a methylene (**16j**) or keto (**16k**) group was used to link the two phenyl rings of **16b**, then there was a decrease in affinity across all four NR2 subunits as well as a decrease in NR2C selectivity, suggesting that the middle ring needs to be a six-membered aromatic ring as found in **16e** for optimal NR2C binding.

To gain insight into the optimal number of phenyl rings required for high NR2 subunit affinity compounds **16a**,**j**,**m**,**n** were synthesized. When one phenyl ring was removed from **16b** to form **16a**, there was a total loss of affinity across all four NR2 subunits. Interestingly, if the first aromatic ring of **16b** was replaced with an (*E*)-ethenyl spacer, then AP5-like subunit selectivity was observed as **16l** displayed the following rank order of affinity: NR2A > NR2B > NR2C > NR2D. A generally similar rank order of affinity was observed for compound **16n**, where the first phenyl ring of **16e** was replaced with an (*E*)-ethenyl substituent. Thus it would appear that the first phenyl ring is essential for NR2C/NR2D vs NR2A/NR2B selectivity. Removal of the last aromatic ring of the phenanthrene ring of **16e** led to compound **16m**, which had a reduced affinity across all four NR2 subunits compared to **16e** but an unusual pattern of selectivity: NR2C > NR2A > NR2B > NR2D. Thus it would appear that all three rings in **16e** contribute to the observed high affinity and NR2C/NR2D selectivity.

Halogen substitution of the biphenyl ring of **16b** resulted in differential effects on NMDA receptor subunit selectivity depending on the position of ring substitution. Thus, 2′-bromo substitution of the biphenyl ring decreased affinity at all NR2 subunits except NR2C, while 4′-fluoro substitution enhanced affinity for NR2A but decreased affinity at NR2B and NR2D. However, 7-bromo substitution (**16g**) had marginal effects on both affinity and pattern of selectivity across all NR2 subunits. In contrast, 7-bromo substitution of compound **16h** led to an enhancement of selectivity for NR2C vs NR2A. Thus, the effects of halogen substitution on NR2 subunit affinity and pattern of selectivity vary depending on the nature of the aromatic substituent and the position of halo substitution on the aromatic ring. This pharmacological heterogeneity may be important in the design of subunit selective antagonists in the future.

Changing the group linking the aromatic substituent to the piperazine ring of **16b** from a carbonyl group to a sulfonyl group (**17**) reduced affinity at NR2B and NR2D, thereby removing the overall NR2B/NR2D selectivity of **16b**. Replacement of the carbonyl linker of **16e** with a methylene group (**23**) led to an ∼30-fold drop in affinity for NR2C and NR2D; however, the pattern of NR2 subunit selectivity was similar to that of **16e**. Thus, a carbonyl linker is preferred over a methylene or sulfonyl group for enhancing potency at NR2D, though for binding to NR2C a methylene group is detrimental but a sulfonyl group is an acceptable linker. The profound difference in affinity observed on replacement of the carbonyl group linker is likely due to the tight restrictions imposed by the hydrophobic binding site in the NR2 subunit on the orientation of the bulky aromatic ring.

The configuration of the carboxylic acid groups on the piperazine ring has a profound influence on subunit selectivity as a cis arrangement in **16e** leads to high affinity across all NR2 subunits and a NR2C/NR2D selectivity while the trans-isomer (**13**) has an ∼60-fold lower affinity for NR2C and NR2D and very little selectivity for NR2C/NR2D vs NR2A/NR2B.

As **16e** was the most potent antagonist identified in this study it was characterized as an antagonist of native NMDA receptors expressed on neonatal rat spinal motoneurones. **16e** was found to be a potent antagonist, and Schild analysis revealed a pA_2 value of 6.45. The Schild plot was a straight line with a slope close to 1 suggestive of a competitive mode of antagonism for **16e**.

We have developed homology models of the S1/S2 domain of NR2 subunits based upon the X-ray crystal structure of the glutamate binding core of the structurally related GluR2 receptor[29] and more recently based on the X-ray crystal structure of NR1.[30] Molecular modeling studies in our laboratory using these homology models suggest that the hydrophobic pocket for bulky aromatic substituents represents the amino acids lining the cleft between the S1 and S2 domains (Kinarsky, L.; et al., submitted). In the case of **16**e, the hydrophobic pocket may represent the groove found in S2 at the base of the 'H' helix[29] that leads directly away from the glutamate binding site, the S1/S2 hinge region, and out toward the surface of the receptor. Most of the NR2 subunit-specific amino acid residues in the area around the glutamate binding pocket are found near the surface of the S1/S2 domain. Thus, only compounds with large aromatic residues can come within reach of the subunit-specific amino acid residues, and this is probably the main reason only antagonists such as **16b**, **16e**, and **5** show altered subunit selectivity compared to more typical AP5-like antagonists. Though the subunit selectivity of **16b**, **16e**, and **16f** is only modest, it might be possible to improve NR2 subunit selectivity by adding substituents to the distal benzene ring of these antagonists to target NR2 subunit specific amino acid residues

around the S1−S2 cleft. Further structure activity relationship studies around the structure of **16e** and **16f** are underway to investigate this theory.

Conclusions

We have developed a synthesis for a series of piperazine-2,3-dicarboxylic acid analogues based on the lead structure **16b**. One compound, **16e**, proved to have much higher affinity for NR2C and NR2D than **16b** and also showed an ~6-fold selectivity for NR2C vs NR2A. A positional isomer of **16e**, **16f**, though less potent than **16e**, had a 7-fold selectivity for NR2D vs NR2B and is therefore a useful lead for the design of NR2D selective antagonists. The compounds synthesized in this study extend previous work showing that NMDA receptor antagonists bearing bulky hydrophobic residues are capable of probing a different part of the antagonist binding pocket, leading to a different subunit selectivity compared to "typical" competitive antagonists such as **2**. It would appear from our studies that for optimal binding to NR2C or NR2D subunits that the bulky hydrophobic residue is preferentially a planar aromatic residue such as a phenanthrene ring.

Though the NR2C vs NR2A selectivity of **16e** is only ~6-fold when this compound is used in combination with NR2A vs NR2D selective antagonists such as **4**, the involvement of individual subunits in physiological processes can begin to be elucidated.[31,32]

Given the NR2C/NR2D subunit selectivity of **16e** and **16f**, they represent leads for the discovery of more potent and NR2 subunit selective antagonists in the future. These will not only be important in elucidating the involvement of NR2C and NR2D subunits in physiological processes in the CNS but may also have therapeutic importance given that at present only NR2A/NR2B or NR2B selective antagonists have been investigated for therapeutic application.

Experimental Section

Chemistry. General Procedures. Proton NMR spectra were measured on a JEOL NMR spectrometer at either 399.78 or 270.18 MHz. Carbon NMR spectra were run on a 399.78 MHz JEOL NMR spectrometer at 100.54 MHz or a 270.18 MHz JEOL spectrometer at 67.94 MHz. 3-(Trimethylsilyl)-propionic-2,2,3,3-d_4 acid, sodium salt in D_2O, or tetramethylsilane in $CDCl_3$ and DMSO-d_6 were used as internal standards. Chemical shifts (δ) are expressed in ppm and coupling constants (J) in Hertz; bs = broad singlet and usp = under solvent peak (chemical shifts correlated via 2D COSY spectra). Elemental analyses were performed in the microanalytical laboratory in the Department of Chemistry, University of Bristol, Bristol, UK. Mass spectrometry was performed in the School of Chemistry at the University of Southampton, Southampton, UK utilizing Electron Ionization (EI) and positive (ES+) and negative (ES-) electrospray ionization techniques. Melting points were determined in capillary tubes on Electrothermal IA9100 electronic melting point equipment and are uncorrected. Thin-layer chromatography was performed on Merck silica gel 60 F254 plastic sheets. Silica gel for flash chromatography was silica gel 60 (220−440 mesh) from Fluka. The eluents for thin-layer chromatography of amino acids included [2 (pyridine:acetic acid:water (3:8:11)):3 (*n*-butanol)] and [propan-2-ol:35% aqueous ammonia (70:30)]. Amino acids were detected by spraying plates with a 2% solution of ninhydrin in 70% ethanol. Ion-exchange resin chromatography was carried out using Dowex 50WX8-400 acid form resin obtained from Aldrich Chemical Co., UK. All reagents and dry solvents were obtained from the Aldrich Chemical Co., unless otherwise stated. The carboxylic acids (**14a**−**n**) were either commercially available or were synthesized by standard methods.

(2*R,3*S**)-Piperazine-2,3-dicarboxylic Acid (7).** Pyrazine-2,3-dicarboxylic acid (**6**) (100 g, 0.595 mol) and potassium hydroxide (66.8 g, 1.19 mol) were dissolved in water (1500 mL) and hydrogenated under 3 atm of hydrogen in the presence of platinum(IV) oxide (1 g) for 3 days. The reaction mixture was filtered through Celite filter agent and concentrated under reduced pressure to a volume of 200 mL. The solution was acidified to pH 3.8 with concentrated nitric acid, yielding a fine white precipitate that was filtered and air-dried to give **7** (57.8 g, 51%) as a white solid. The filtrate was concentrated under reduced pressure and applied to a column of Dowex 50WX8-400 resin H^+ form (100 mL). The column was eluted with water until the eluent had a pH of 5 and then the product was eluted with 10% aqueous ammonia solution. The ninhydrin-positive fractions were combined and evaporated to dryness under reduced pressure. The solid was purified by crystallization from boiling water to give a further 48.4 g (42%) of **7**: mp 295−298 °C (dec); ^{1}H NMR (400 MHz, D_2O/NaOD, pH 11) δ 2.67 (m, 2H, HNCH_2), 2.78 (m, 2H, HNCH_2), 3.53 (s, 2H, HNCHCO_2H); ^{13}C NMR (100 MHz, D_2O/NaOD, pH 11) δ 45.34, 62.23, 181.34; MS (ES-) m/z = 173.1 (M − H). Anal. ($C_6H_{10}N_2O_4 \cdot H_2O$) C, H, N.

(2*R,3*S**)-1,4-Dibenzylpiperazine-2,3-dicarboxylic Acid Diethyl Ester (10).** A solution of *N*,*N*-dibenzylethylene-1,2-diamine (**9**) (48.3 g, 0.2 mol) and triethylamine (40.5 g, 0.4 mol) in anhydrous benzene (50 mL) was added dropwise to a mechanically stirred solution of 2,3-dibromosuccinic acid diethyl ester (**8**)[20] (66.4 g, 0.2 mol) in anhydrous benzene (160 mL) at 40 °C under a dry argon atmosphere. The reaction mixture was heated to 80 °C and stirred for a further 3 h. Upon cooling the reaction mixture was filtered to remove triethylamine hydrobromide. The filtrate was washed with water, dried ($MgSO_4$), and concentrated under reduced pressure. The crude product was preabsorbed onto silca gel and flash chromatographed over silica gel. Elution with petroleum ether/diethyl ether (9:1) yielded an off white crystalline solid. Crystallization from absolute ethanol gave **10** (26.1 g, 32%) as a white crystalline solid: mp 91−92 °C (dec); ^{1}H NMR (400 MHz, $CDCl_3$) δ 1.23 (t, J = 6.9 Hz, 6H, CH_3), 2.53 (d, $J_{A,B}$ = 7.3 Hz, 2H, BnNCH_2), 3.29 (d, J_{BA} = 7.3 Hz, 2H, BnNCH_2), 3.89 (s, 2H, NCHCO_2Et), 3.93 (s, 4H, ArCH_2N), 4.18 (m, 4H, CO_2CH_2CH_3), 7.23 (m, 10H, Ar); ^{13}C NMR (100 MHz, $CDCl_3$) δ 14.10, 46.51, 59.21, 60.09, 62.63, 126.82, 127.99, 128.49, 138.89, 170.72; MS (EI) m/z = 410 (M+), 337, 264, 173, 91. Anal. ($C_{24}H_{30}N_2O_4$) C, H, N.

(2*R,3*R**)-Piperazine-2,3-dicarboxylic Acid Diethyl Ester (11).** (2*R**,3*R**)-1,4-Dibenzylpiperazine-2,3-dicarboxylic acid diethyl ester (**10**) (6.5 g, 16 mmol) was dissolved in anhydrous ethanol (100 mL) and stirred under an atmosphere of hydrogen in the presence of 10 wt % palladium on activated carbon (0.5 g). The reaction mixture was filtered through Celite filter agent, and solvents were removed under reduced pressure. The crude product was flash chromatographed over silica gel; elution first with diethyl ether removed a trace impurity and then the product was eluted with ethyl acetate/methanol (9:1). The eluent was evaporated to dryness under reduced pressure, and the product was redissolved in diethyl ether, filtered to remove traces of silica gel, and then evaporated to dryness under reduced pressure to yield **11** (3.0 g, 82%) as an amber colored oil: ^{1}H NMR (270 MHz, $CDCl_3$) δ 1.30 (t, J = 7.3 Hz, 6H, CH_3), 2.02 (bs, 2H, NH), 2.74 (d, J = 8.6 Hz, 2H, HNCH_2), 3.00 (d, J = 8.6 Hz, 2H, HNCH_2), 3.81 (s, 2H, HNCHCO_2Et), 4.24 (m, 4H, CO_2CH_2CH_3); ^{13}C NMR (100 MHz, $CDCl_3$) δ 13.55, 43.47, 58.57, 60.51, 170.35; MS (ES+) m/z = 231.2 (MH^+). Anal. ($C_{10}H_{18}N_2O_4$) C, H, N.

(2*R,3*R**)-Piperazine-2,3-dicarboxylic Acid (12).** (2*R**,3*R**)-Piperazine-2,3-dicarboxylic acid diethyl ester (**11**) (3 g, 13 mmol) and sodium hydroxide (2 g, 50 mmol) were stirred in absolute ethanol for 12 h. Solvents were removed under reduced pressure. The residue was redissolved in 20 mL of

water and the pH of the solution was adjusted to 3.8 with concentrated nitric acid. Dowex 50WX8-400 resin H^+ form (10 mL) was added and the mixture was stirred for 30 min. The slurry was then applied to a column of Dowex 50WX8-400 resin H^+ form (10 mL) and the column was eluted with water until the eluent had a pH of 5. The product was eluted with 10% aqueous ammonia solution, and the ninhydrin-positive fractions were combined and evaporated to dryness under reduced pressure. The solid was purified by crystallization from boiling water to give **12** (1.8 g, 78%) as a white solid: mp 283−285 °C (dec); ^{1}H NMR (400 MHz, D_2O/NaOD, pH 11) δ 2.69 (m, 2H, NHCH_2), 2.90 (m, 2H, NHCH_2), 3.25 (s, 2H, NHCHCO_2H); ^{13}C NMR (100 MHz, D_2O/NaOD, pH 11) δ 46.23, 65.79, 181.07; MS (ES-) m/z = 173.1 (M − H). Anal. ($C_6H_{10}N_2O_4\cdot H_2O$) C, H, N.

General Procedure for Preparing Acid Chlorides (15a−n). The carboxylic acid (**14a−n**) (10 mmol) was refluxed with excess thionyl chloride (5 mL) in anhydrous benzene (50 mL) under a dry argon atmosphere for up to 12 h. Once all the carboxylic acid had dissolved, the solution was allowed to cool and was evaporated to dryness under reduced pressure. The product was redissolved in a second aliquot of anhydrous benzene (50 mL) and this was again evaporated to dryness under reduced pressure, ensuring complete removal of any excess thionyl chloride. The acid chlorides (**15a−n**) were used without any further purification.

General Procedure for Coupling of Acid Chloride (15a−n) and Piperazine-2,3-dicarboxylic Acid (7 or 12). A solution of the acid chloride (**15a−n**) (1 equiv) in dioxane (20 mL) was added dropwise to a rapidly stirring solution of the piperazine-2,3-dicarboxylic acid (**7** or **12**) (1 equiv) and sodium hydroxide (3 equiv) dissolved in water/dioxane (1:1) at 0 °C. The reaction mixture was stirred at 0 °C for 2 h and then allowed to warm to room temperature and stirred for a further 3 h. The pH of the reaction mixture was adjusted to 7, diluted to twice the volume with water, and reduced to half volume under reduced pressure. The reaction mixture was acidified to pH 3 with 2 M aqueous hydrochloric acid, and the precipitate formed was filtered and washed with water and then three times with hot dioxane. The solid was redissolved in a minimum volume of aqueous sodium hydroxide, filtered, and then precipitated with 2 M aqueous hydrochloric acid at a pH of 3. The precipitate was washed with water and air-dried.

(2*R,3*S**)-1-Benzoylpiperazine-2,3-dicarboxylic Acid (16a).** Acid chloride **15a** (1.46 g, 10.4 mmol) in dioxane (40 mL) and (2*R**,3*S**)-piperazine-2,3-dicarboxylic acid (**7**) (2.00 g, 10.4 mmol) and sodium hydroxide (0.83 g, 31.2 mmol) in water/dioxane (1:1) (40 mL) gave a solid that was washed with ethanol followed by diethyl ether to yield the monosodium salt of **16a** (2.0 g, 52%) as white fluffy crystals: mp 255−258 °C (dec); ^{1}H NMR (270 MHz, D_2O/NaOD, pH 11) δ 2.60−2.85 (m, 1H, HNCH_2), 2.88−3.05 (m, 1H, HNCH_2), 3.10−3.23 (m, 1H, CONCH_2), 3.31 (d, J = 3.6 Hz, 0.5H, HNCHCO_2H), 3.37 (d, J = 3.6 Hz, 0.5H, HNCHCO_2H), 3.55 (d, J = 13.5 Hz, 0.5H, CONCH_2), 4.33 (d, J = 13.5 Hz, 0.5H, CONCH_2), 4.69 (d, J = 3.6 Hz, 0.5H, CONCHCO_2H), 5.53 (d, J = 3.6 Hz, 0.5H, CONCHCO_2H), 7.54 (m, 5H, Ar); MS (ES+) m/z = 279.2 (M + H), 301.2 (M + H + Na), 323.2 (M + H + 2Na). Anal. ($C_{13}H_{13}N_2O_5Na\cdot 4H_2O$) C, H, N.

(2*R,3*S**)-(Biphenylyl-4-carbonyl)piperazine-2,3-dicarboxylic Acid (16b).** Acid chloride **15b** (2.00 g, 9.2 mmol) in dioxane (40 mL) and (2*R**,3*S**)-piperazine-2,3-dicarboxylic acid (**7**) (1.77 g, 9.2 mmol) and sodium hydroxide (1.11 g, 27.7 mmol) in water/dioxane (1:1) (40 mL) gave **16b** (1.21 g, 31%) as a white solid: mp 204−206 °C (dec); ^{1}H NMR (270 MHz, D_2O/NaOD, pH 11) δ 2.54−3.06 (m, 2H, HNCH_2), 3.10−3.24 (m, 1H, CONCH_2), 3.33 (d, J = 3.6 Hz, 0.5H, HNCHCO_2H), 3.35 (d, J = 3.6 Hz, 0.5H, HNCHCO_2H), 3.57 (d, J = 13.9 Hz, 0.5H, CONCH_2), 4.35 (d, J = 13.9 Hz, 0.5H, CONCH_2), 4.75 (d, J = 3.6 Hz, 0.5H, CONCHCO_2H), 5.58 (d, J = 3.6 Hz, 0.5H, CONCHCO_2H), 7.40−7.79 (m, 8H, Ar); MS (ES+) m/z = 355.3 (M + H), 377.2 (M + H + Na), 399.2 (M + H + 2Na). Anal. ($C_{19}H_{18}N_2O_5\cdot 2H_2O$) C, H, N.

(2*R,3*S**)-1-(2′-Bromobiphenylyl-4-carbonyl)piperazine-2,3-dicarboxylic Acid (16c).** Acid chloride **15c** (5.17 g, 17.5 mmol) in dioxane (50 mL) and (2*R**,3*S**)-piperazine-2,3-dicarboxylic acid (**7**) (3.05 g, 15.9 mmol) and sodium hydroxide (1.91 g, 47.7 mmol) in water/dioxane (1:1) (50 mL) gave **16c** (1.16 g, 15%) as a white solid: mp 238−240 °C (dec); ^{1}H NMR (270 MHz, D_2O/NaOD, pH 11) δ 2.63−2.84 (m, 1H, HNCH_2), 2.91−3.07 (m, 1H, HNCH_2), 3.12−3.28 (m, 1H, CONCH_2), 3.35 (d, J = 3.6 Hz, 0.5H, HNCHCO_2H), 3.39 (d, J = 3.6 Hz, 0.5H, HNCHCO_2H), 3.62 (d, J = 13.2 Hz, 0.5H, CONCH_2), 4.36 (d, J = 13.2 Hz, 0.5H, CONCH_2), 4.82 (usp, 0.5H, CONCHCO_2H), 5.54 (d, J = 3.6 Hz, 0.5H, CONCHCO_2H), 7.31−7.38 (m, 1H, Ar), 7.41−7.53 (m, 2H, Ar), 7.54−7.64 (m, 4H, Ar), 7.78 (d, J = 7.9 Hz, 1H, Ar); MS (ES+) m/z = 434.2, 435.2 (M + H), 455.2. 457.2 (M + H + Na). Anal. ($C_{19}H_{17}N_2O_5Br$) C, H, N.

(2*R,3*S**)-1-(4′-Fluorobiphenylyl-4-carbonyl)piperazine-2,3-dicarboxylic Acid (16d).** Acid chloride **15d** (9.32 g, 39.7 mmol) in dioxane (100 mL) and (2*R**,3*S**)-piperazine-2,3-dicarboxylic acid (**7**) (7.62 g, 39.7 mmol) and sodium hydroxide (4.76 g, 0.12 mol) in water/dioxane (1:1) (100 mL) gave the monosodium salt of **16d** (3.58 g, 20%) as a white solid: mp 258−263 °C (dec); δ 2.63−2.83 (m, 1H, HNCH_2), 2.90−3.05 (m, 1H, HNCH_2), 3.11−3.27 (m, 1H, CONCH_2), 3.34 (d, J = 3.6 Hz, 0.5H, HNCHCO_2H), 3.39 (d, J = 3.6 Hz, 0.5H, HNCHCO_2H), 3.57 (d, J = 13.2 Hz, 0.5H, CONCH_2), 4.35 (d, J = 13.2 Hz, 0.5H, CONCH_2), 4.77 (d, J = 3.6 Hz, 0.5H, CONCHCO_2H), 5.53 (d, J = 3.6 Hz, 0.5H, CONCHCO_2H), 7.21−7.30 (m, 2H, Ar), 7.55−7.63 (m, 2H, Ar), 7.67−7.78 (m, 4H, Ar); MS (ES+) m/z = 373.2 (M + H), 395.2 (M + H + Na). Anal. ($C_{19}H_{16}N_2O_5FNa\cdot 2.75H_2O$) C, H, N.

(2*R,3*S**)-1-(Phenanthrenyl-2-carbonyl)piperazine-2,3-dicarboxylic Acid (16e).** Acid chloride **15e** (10.80 g, 45.0 mmol) in dioxane (100 mL) and (2*R**,3*S**)-piperazine-2,3-dicarboxylic acid (**7**) (8.64 g, 45.0 mmol) and sodium hydroxide (5.40 g, 0.13 mol) in water/dioxane (1:1) (100 mL) gave **16e** (5.84 g, 30%) as a white solid; mp 223−226 °C (dec);^{1}H NMR (270 MHz, D_2O/NaOD, pH 11) δ 2.62−3.29 (m, 3H, HNCH_2, CONCH_2), 3.38 (d, J = 3.6 Hz, 0.5H, HNCHCO_2H), 3.43 (d, J = 3.6 Hz, 0.5H, HNCHCO_2H), 3.54 (d, J = 13.9 Hz, 0.5H, CONCH_2), 4.43 (d, J = 13.9 Hz, 0.5H, CONCH_2), 4.79 (usp, 0.5H, CONCHCO_2H), 5.60 (d, J = 3.6 Hz, 0.5H, CONCHCO_2H), 7.63−8.12 (m, 7H, Ar), 8.58−8.79 (m, 2H, Ar); MS (ES-) m/z = 377.2 (M − H), 399.2 (M − H + Na). Anal. ($C_{21}H_{18}N_2O_5\cdot 3.0H_2O$) C, H, N.

(2*R,3*S**)-1-(Phenanthrenyl-3-carbonyl)piperazine-2,3-dicarboxylic Acid (16f).** Acid chloride **15f** (2.16 g, 9.0 mmol) in dioxane (40 mL) and (2*R**,3*S**)-piperazine-2,3-dicarboxylic acid (**7**) (1.73 g, 9.0 mmol) and sodium hydroxide (1.08 g, 27.0 mmol) in water/dioxane (1:1) (40 mL) gave **16f** (410 mg, 12%) as a white solid: mp 205−208 °C (dec); ^{1}H NMR (270 MHz, D_2O/NaOD, pH 11) δ 2.45−2.59 (m, 0.5H, HNCH_2), 2.68−2.92 (m, 1H, HNCH_2), 3.03−3.26 (m, 1.5H, CONCH_2, HNCH_2), 3.30−3.42 (m, 1.5H, CONCH_2, HNCHCOOH), 4.45 (d, J = 12.5 Hz, 0.5H, CONCH_2), 4.80 (usp, 0.5H, CONCHCOOH), 5.59 (d, J = 3.6 Hz, 0.5H, CONCHCOOH), 7.42−7.85 (m, 6.5H, Ar), 7.98 (d, J = 8.6 Hz, 0.5H, Ar), 8.51 (d, J = 8.2 Hz, 0.5H, Ar), 8.61 (d, J = 8.2 Hz, 0.5H, Ar), 8.65 (s, 0.5H, Ar), 8.87 (s, 0.5H, Ar); MS (ES+) m/z = 379.2 (M + H), 401.2 (M + Na), 423.2 (M + 2Na). Anal. ($C_{21}H_{18}N_2O_5\cdot H_2O$) C, H, N.

(2*R,3*S**)-1-(7-Bromophenanthrenyl-2-carbonyl)piperazine-2,3-dicarboxylic Acid (16g).** Acid chloride **15g** (1.06 g, 3.3 mmol) in dioxane (40 mL) and (2*R**,3*S**)-piperazine-2,3-dicarboxylic acid (**7**) (0.64 g, 3.3 mmol) and sodium hydroxide (0.40 g, 9.9 mmol) in water/dioxane (1:1) (40 mL) gave **16g** (163 mg, 11%) as a brown solid: mp 225−228 °C (dec); ^{1}H NMR (270 MHz, D_2O/NaOD, pH 11) δ 2.58−2.72 (m, 0.5H, HNCH_2), 2.80−2.97 (m, 1H, CONCH2, HNCH_2), 3.00−3.12 (m, 0.5H, HNCH_2), 3.18−3.31 (m, 1H, CONCH_2), 3.40−3.51 (m, 1.5H, CONCH_2, HNCHCO_2H), 4.43 (d, J = 12.5 Hz, 0.5H, CONCH_2), 4.89 (d, J = 3.6 Hz, 0.5H, CONCHCO_2H), 5.60 (d, J = 3.6 Hz, 0.5H, CONCHCO_2H), 7.06 (d, J = 8.6 Hz, 0.5H, Ar), 7.21 (d, J = 8.6 Hz, 0.5H, Ar), 7.27 (d, J = 8.9 Hz, 0.5H, Ar), 7.34−7.85 (m, 4.5H, Ar), 7.96−8.11 (m, 1.5H, Ar), 8.33 (d, J = 7.9

Hz, 0.5H, Ar); MS (ES+) *m/z* = 457.2, 459.1 (M + H), 479.2, 481.1 (M + H + Na). Anal. ($C_{21}H_{17}N_2O_5Br\cdot 2.0H_2O$) C, H, N.

(2*R,3*S**)-(9,10-Dihydrophenanthrenyl-2-carbonyl)-piperazine-2,3-dicarboxylic Acid (16h).** Acid chloride **15h** (2.15 g, 8.9 mmol) in dioxane (40 mL) and (2*R**,3*S**)-piperazine-2,3-dicarboxylic acid (**7**) (1.71 g, 8.9 mmol) and sodium hydroxide (1.07 g, 26.7 mmol) in water/dioxane (1:1) (40 mL) gave **16h** (252 mg, 7%) as a white solid: mp 205−208 °C (dec); ^{1}H NMR (270 MHz, D_2O/NaOD, pH 11) δ 2.61−2.83 (m, 1H, HNCH_2), 2.87 (s, 2H, ArCH_2CH_2Ar), 2.89 (s, 2H, ArCH_2CH_2Ar), 2.94−3.07 (m, 1H, HNCH_2), 3.11−3.26 (m, 1H, CONCH_2), 3.32 (d, J = 3.6 Hz, 0.5H, HNC*H*CO$_2$H), 3.37 (d, J = 3.6 Hz, 0.5H, HNC*H*CO$_2$H), 3.59 (d, J = 13.9 Hz, 0.5H, CONCH_2), 4.34 (d, J = 13.9 Hz, 0.5H, CONCH_2), 4.84 (usp, 0.5H, CONC*H*CO$_2$H), 5.53 (d, J = 3.6 Hz, 0.5H, CONC*H*CO$_2$H), 7.33−7.49 (m, 5H, Ar), 7.85−7.94 (m, 1H, Ar); MS (ES+) *m/z* = 381.3 (M + H), 403.3 (M + H + Na), 425.3 (M + H + 2Na). Anal. ($C_{21}H_{20}N_2O_5\cdot H_2O$) C, H, N.

(2*R,3*S**)-1-(7-Bromo-9,10-dihydrophenanthrenyl-2-carbonyl)piperazine-2,3-dicarboxylic Acid (16i).** Acid chloride **15i** (1.06 g, 3.3 mmol) in dioxane (40 mL) and (2*R**,3*S**)-piperazine-2,3-dicarboxylic acid (**7**) (0.63 g, 3.3 mmol) and sodium hydroxide (0.40 g, 9.9 mmol) in water/dioxane (1:1) (40 mL) gave **16i** (190 mg, 11%) as a white solid: mp 209−211 °C (dec); ^{1}H NMR (270 MHz, D_2O/NaOD, pH 11) δ 2.63−2.88 (m, 5H, ArCH_2CH_2Ar, HNCH_2), 2.91−3.06 (m, 1H, HNCH_2), 3.10−3.28 (m, 1H, CONCH_2), 3.32 (d, J = 3.6 Hz, 0.5H, HNC*H*CO$_2$H), 3.38 (d, J = 3.6 Hz, 0.5H, HNC*H*CO$_2$H), 3.59 (d, J = 13.5 Hz, 0.5H, CONCH_2), 4.34 (d, J = 13.5 Hz, 0.5H, CONCH_2), 4.75 (d, J = 3.6 Hz, 0.5H, CONC*H*CO$_2$H), 5.52 (d, J = 3.6 Hz, 0.5H, CONC*H*CO$_2$H), 7.37−7.53 (m, 4H, Ar), 7.66 (d, J = 8.9 Hz, 0.5H, Ar), 7.72 (d, J = 8.9 Hz, 0.5H, Ar), 7.80 (d, J = 7.9 Hz, 0.5H, Ar), 7.86 (d, J = 7.9 Hz, 0.5H, Ar); MS (ES+) *m/z* = 459.2 (M + H), 482.2 (M + H + Na), 505.2 (M + H + 2Na). Anal. ($C_{21}H_{19}N_2O_5Br\cdot 3.0H_2O$) C, H, N.

(2*R,3*S**)-1-(9*H*-Fluorenyl-2-carbonyl)piperazine-2,3-dicarboxylic Acid (16j).** Acid chloride **15j** (2.17 g, 9.5 mmol) in dioxane (40 mL) and (2*R**,3*S**)-piperazine-2,3-dicarboxylic acid (**7**) (1.83 g, 9.5 mmol) and sodium hydroxide (1.14 g, 28.6 mmol) in water/dioxane (1:1) (40 mL) gave **16j** (440 mg, 12%) as a pale yellow solid: mp 230−233 °C (dec); ^{1}H NMR (270 MHz, D_2O/NaOD, pH 11) δ 2.66−2.84 (m, 1H, HNCH_2), 2.89−3.06 (m, 1H, HNCH_2), 3.11−3.28 (m, 1H, CONCH_2), 3.34 (d, J = 3.6 Hz, 0.5H, HNC*H*CO$_2$H), 3.39 (d, J = 3.6 Hz, 0.5H, HNC*H*CO$_2$H), 3.60 (d, J = 13.2 Hz, 0.5H, CONCH_2), 3.91 (m, 2H, ArCH_2Ar), 4.36 (d, J = 13.2 Hz, 0.5H, CONCH_2), 4.81 (usp, 0.5H, CONC*H*CO$_2$H), 5.54 (d, J = 3.3 Hz, 0.5H, CONC*H*CO$_2$H), 7.33−7.72 (m, 5.5H, Ar), 7.79−7.95 (m, 1.5H, Ar); MS (ES+) *m/z* = 367.3 (M + H), 389.3 (M + H + Na), 411.2 (M + H + 2Na). Anal. ($C_{20}H_{18}N_2O_5\cdot 0.5H_2O$) C, H, N.

(2*R,3*S**)-1-(9-Oxo-9*H*-fluorenyl-2-carbonyl)piperazine-2,3-dicarboxylic Acid (16k).** Acid chloride **15k** (0.84 g, 3.5 mmol) in dioxane (20 mL) and (2*R**,3*S**)-piperazine-2,3-dicarboxylic acid (**7**) (0.5 g, 2.6 mmol) and sodium hydroxide (0.31 g, 7.8 mmol) in water/dioxane (1:1) (20 mL) gave **16k** (89 mg, 7%) as a pale yellow solid: mp 225−228 °C (dec); ^{1}H NMR (270 MHz, D_2O/NaOD, pH 11) δ 2.71−2.85 (m, 1H, HNCH_2), 2.91−3.36 (m, 2H, CONCH_2, HNCH_2), 3.38 (d, J = 3.6 Hz, 0.5H, HNC*H*CO$_2$H), 3.41 (d, J = 3.6 Hz, 0.5H, HNC*H*CO$_2$H), 3.60 (d, J = 13.5 Hz, 0.5H, CONCH_2), 4.34 (d, J = 13.5 Hz, 0.5H, CONCH_2), 4.78 (d, J = 3.6 Hz, 0.5H, CONC*H*CO$_2$H), 5.53 (d, J = 3.6 Hz, 0.5H, CONC*H*CO$_2$H), 7.16−7.28 (m, 2H, Ar), 7.31−7.46 (m, 3H, Ar), 7.52−7.65 (m, 2H, Ar); MS (ES+) *m/z* = 381.2 (M + H), 403.2 (M + H + Na), 425.2 (M + H + 2Na). Anal. ($C_{20}H_{16}N_2O_6\cdot 0.7H_2O$) C, H, N.

(2*R,3*S**,*E*)-(3-Phenylacryloyl)piperazine-2,3-dicarboxylic Acid (16l).** Acid chloride **15l** (0.57 g, 3.5 mmol) in dioxane (20 mL) and (2*R**,3*S**)-piperazine-2,3-dicarboxylic acid (**7**) (0.50 g, 2.6 mmol) and sodium hydroxide (0.31 g, 7.8 mmol) in water/dioxane (1:1) (20 mL) gave **16l** (288 mg, 26%) as a white solid: mp 251−253 °C (dec); ^{1}H NMR (270 MHz, D_2O/NaOD, pH 11) δ 2.61−2.87 (m, 1.5H, HNCH_2), 3.05−3.31 (m, 1.5H, CONCH_2, HNCH_2), 3.27 (d, J = 3.6 Hz, 0.5H, HNC*H*CO$_2$H), 3.34 (d, J = 3.6 Hz, 0.5H, HNC*H*CO$_2$H), 4.04 (d, J = 13.5 Hz, 0.5H, CONCH_2), 4.31 (d, J = 13.5 Hz, 0.5H, CONCH_2), 4.77 (d, J = 3.6 Hz, 0.5H, CONC*H*CO$_2$H), 5.53 (d, J = 3.6 Hz, 0.5H, CONC*H*CO$_2$H), 7.12 (d, 0.5H, J = 15.8 Hz, H_{vic}), 7.24 (d, 0.5H, J = 15.8 Hz, H_{vic}), 7.45−7.51 (m, 2.5H, Ar), 7.58 (d, 0.5H, J = 15.8 Hz, H_{vic}), 7.60 (d, 0.5H, J = 15.8 Hz, H_{vic}), 7.65−7.74 (m, 2.5H, Ar); MS (ES+) *m/z* = 305.3 (M + H), 327.2 (M + H + Na), 349.2 (M + H + 2Na). Anal. ($C_{15}H_{16}N_2O_5\cdot H_2O$) C, H, N.

(2*R,3*S**)-1-(Naphthalenyl-2-carbonyl)piperazine-2,3-dicarboxylic Acid (16m).** Acid chloride (**15m**) (2.0 g, 10.5 mmol) in dioxane (40 mL) and (2*R**,3*S**)-piperazine-2,3-dicarboxylic acid (**7**) (2.01 g, 10.5 mmol) and sodium hydroxide (1.26 g, 31.5 mmol) in water/dioxane (1:1) (40 mL) gave the monosodium salt of **16m** (1.41 g, 37%) as a white solid: mp 250−253 °C (dec); ^{1}H NMR (270 MHz, D_2O/NaOD, pH 11) δ 2.66−2.87 (m, 1H, HNCH_2), 2.89−3.09 (m, 1H, HNCH_2), 3.13−3.28 (m, 1H, CONCH_2), 3.35 (d, J = 3.6 Hz, 0.5H, HNC*H*CO$_2$H), 3.43 (d, J = 3.6 Hz, 0.5H, HNC*H*CO$_2$H), 3.59 (d, J = 13.9 Hz, 0.5H, CONCH_2), 4.40 (d, J = 13.9 Hz, 0.5H, CONCH_2), 4.78 (usp, 0.5H, CONC*H*CO$_2$H), 5.58 (d, J = 3.6 Hz, 0.5H, CONC*H*CO$_2$H), 7.58−7.70 (m, 3H, Ar), 8.00−8.11 (m, 4H, Ar); MS (ES+) *m/z* = 329.2 (M + H), 351.2 (M + H + Na), 373.2 (M + H + 2Na). Anal. ($C_{17}H_{15}N_2O_5\cdot H_2O$) C, H, N.

(2*R,3*S**,*E*)-1-(3-Naphthalen-2-ylacryloyl)piperazine-2,3-dicarboxylic Acid (16n).** Acid chloride **15n** (1.13 g, 5.2 mmol) in dioxane (40 mL) and (2*R**,3*S**)-piperazine-2,3-dicarboxylic acid (**7**) (1.00 g, 5.2 mmol) and sodium hydroxide (0.63 g, 15.6 mmol) in water/dioxane (1:1) (40 mL) gave **16n** (530 mg, 31%) as a white solid: mp 285−287 °C (dec); ^{1}H NMR (270 MHz, D_2O/NaOD, pH 11) δ 2.59−2.84 (m, 1.5H, HNCH_2), 3.20−3.30 (m, 1.5H, HNC*H*CO$_2$H, CONCH_2), 3.98 (d, J = 13.4 Hz, 0.5H, CONCH_2), 4.36 (d, J = 13.4 Hz, 0.5H, CONCH_2), 5.17 (d, J = 3.6 Hz, 0.5H, CONC*H*CO$_2$H), 5.52 (d, J = 3.6 Hz, 0.5H, CONC*H*CO$_2$H), 7.06 (d, J = 15.1 Hz, 0.5H, H_{vic}), 7.23 (d, J = 15.1 Hz, 0.5H, H_{vic}), 7.53−8.04 (m, 8H, Ar, H_{vic}); MS (ES+) *m/z* = 355.2 (M + H), 377.2 (M + H + Na), 399.2 (M + H + 2Na). Anal. ($C_{19}H_{18}N_2O_5\cdot 1.5H_2O$) C, H, N.

(2*R,3*S**)-1-(Biphenylyl-4-sulfonyl)piperazine-2,3-dicarboxylic Acid (17).** Biphenyl-4-sulfonyl chloride (1.32 g, 5.2 mmol) in dioxane (40 mL) and (2*R**,3*S**)-piperazine-2,3-dicarboxylic acid (**7**) (1.00 g, 5.2 mmol) and sodium hydroxide (0.63 g, 15.6 mmol) in water/dioxane (1:1) (40 mL) gave **17** (1.61 g, 37%) as a white solid: mp 198−200 °C (dec); ^{1}H NMR (270 MHz, D_2O/NaOD, pH 11) 2.22−2.39 (m, 1H, HNCH_2), 2.84 (d, J = 13.9 Hz, 1H, OSONCH_2), 3.12 (d, J = 3.0 Hz, 1H, HNC*H*CO$_2$H), 3.18−3.32 (m, 1H, HNCH_2), 4.42 (d, J = 13.9 Hz, 1H, OSONCH_2), 4.80 (d, J = 3.0 Hz, 1H, OSONC*H*CO$_2$H), 7.22−7.37 (m, 5H, Ar), 7.45 (d, J = 8.4 Hz, 2H, Ar), 7.76 (d, J = 8.4 Hz, 2H, Ar); MS (ES+) *m/z* = 391.2 (M + H), 413.1 (M + H + Na). Anal. ($C_{18}H_{18}N_2O_6S\cdot 1.5H_2O$) C, H, N.

(2*R,3*R**)-1-(Phenanthrenyl-2-carbonyl)piperazine-2,3-dicarboxylic Acid (13).** Acid chloride **15e** (1.08 g, 4.5 mmol) in dioxane (40 mL) and (2*R**,3*R**)-piperazine-2,3-dicarboxylic acid (**12**) (0.78 g, 4.5 mmol) and sodium hydroxide (0.54 g, 13.5 mmol) in water/dioxane (1:1) (40 mL) gave **13** (295 mg, 17%) as a white solid: mp 250−252 °C (dec); ^{1}H NMR (270 MHz, D_2O/NaOD pH 11) δ 2.63−3.11 (m, 2.0H, HNCH_2), 3.26−3.60 (m, 1.5H, CONCH_2), 3.93 (d, J = 1.3 Hz, 0.5H, HNC*H*CO$_2$H), 4.17 (d, J = 1.3 Hz, 0.5H, HNC*H*CO$_2$H), 4.41 (d, J = 13.5 Hz, 0.5H, CONCH_2), 4.86 (d, J = 1.3 Hz, 0.5H, CONC*H*CO$_2$H), 5.65 (d, J = 1.3 Hz, 0.5H, CONC*H*CO$_2$H), 7.69−7.80 (m, 3H, Ar), 7.87−7.91 (m, 2H, Ar), 7.99−8.08 (m, 2H, Ar), 8.76−8.88 (m, 2H, Ar); MS (ES+) *m/z* = 379.3 (M + H), 401.2 (M + H + Na), 423.2 (M + H + 2Na). Anal. ($C_{21}H_{18}N_2O_5\cdot 3.0H_2O$) C, H, N.

2-Iodomethylphenanthrene (19). To a stirring solution of 2-hydroxymethylphenanthrene (**18**)[21] (4.2 g, 20 mmol) in anhydrous dioxane (100 mL) at room temperature under an argon atmosphere were added potassium iodide (3.35 g, 20 mmol) and boron trifluoride diethyl etherate (2.86 g, 20 mmol). After stirring for 12 h the solution was diluted with 200 mL of diethyl ether and washed with a 10% sodium metabisulfite solution (100 mL) followed by water (2 × 100 mL). The organics were dried over magnesium sulfate and concentrated to yield

19 (6.0 g, 94%) as an off-white powder: mp 81−83 °C (dec); ^{1}H NMR (270 MHz, $CDCl_3$) δ 4.65 (s, 2H, ICH_2Ar), 7.55−7.88 (m, 7H, Ar), 8.60 (m, 2H, Ar); MS (EI) m/z = 318 (M^+), 191 ($M^+ - I$). Anal. ($C_{15}H_{11}I$) C, H, N.

(2*R,3*S**)-Piperazine-2,3-dicarboxylic Acid Dimethyl Ester (21).** Pyrazine-2,3-dicarboxylic acid dimethyl ester (**20**) (2.0 g, 10 mmol) was dissolved in anhydrous ethanol (30 mL) and stirred under an atmosphere of hydrogen in the presence of 10 wt % palladium on activated carbon for 24 h. The reaction mixture was filtered through Celite filter agent and concentrated under reduced pressure. The crude product was flash chromatographed over silica gel with ethyl acetate as the eluent, which removed impurities, followed by methanol, which eluted the product. The eluent was evaporated to dryness under reduced pressure, and the product was redissolved in diethyl ether, filtered to remove traces of silica gel, and then evaporated to dryness under reduced pressure to yield **21** (1.6 g, 78%) as a viscous amber oil: ^{1}H NMR (270 MHz, $CDCl_3$) δ 2.54 (2H, NH, bs), 2.75−2.96 (4H, CH_2, m), 3.76 (6H, CH_3, s), 3.90 (2H, CH, s); ^{13}C NMR (270 MHz, $CDCl_3$) δ 44.00, 51.85, 58.48, 171.37; MS (ES+) m/z = 203.1 (MH^+). Anal. ($C_8H_{14}N_2O_4$) C, H, N.

(2*R,3*S**)-1-Phenanthren-2-ylmethylpiperazine-2,3-dicarboxylic Acid Dimethyl Ester (22).** A solution of 2-iodomethylphenanthrene (**19**) (0.79 g, 2.5 mmol) in tetrahydrofuran (10 mL) was added dropwise to a stirred solution of (2*R**,3*S**)-piperazine-2,3-dicarboxylic acid dimethyl ester (**21**) (1.0 g, 5.0 mmol) and triethylamine (0.25 g, 2.5 mmol) in tetrahydrofuran (30 mL) at 0 °C for 2 h. The solution was allowed to warm to room temperature and continued to stir for 12 h. Solvents were removed under reduced pressure, and the residue was redissolved in ethyl acetate (50 mL). The organics were washed with water (2 × 50 mL), dried over magnesium sulfate, and concentrated. The crude product was flash chromatographed over silica gel with ethyl acetate as the eluent. The eluted product was evaporated to dryness under reduced pressure, and the product was redissolved in diethyl ether, filtered to remove traces of silica gel, and then evaporated to dryness under reduced pressure to yield **22** (0.5 g, 51%) as an amber solid: mp 116−117 °C; ^{1}H NMR (270 MHz, $CDCl_3$) δ 2.11 (bs, 1H, NH), 2.54 (m, 1H, HNCH_2), 2.90 (m, 2H, HNCH_2, HNCH_2CH_2), 3.06 (m, 1H, HNCH_2CH_2), 3.70 (s, 1H, CH_3), 3.73 (s, 1H, CH_3), 3.86 (d, J = 3.6 Hz, 1H, HNCHCO_2CH_3), 3.93 (d, J = 3.6 Hz, 1H, NCHCO_2CH_3), 3.97 (d, $J_{A,B}$ = 13.9 Hz, 1H, NCH_2Ar), 4.08 (d, $J_{B,A}$ = 13.9 Hz, 1H, NCH_2Ar), 7.53−7.75 (m, 5H, Ar), 7.79 (s, 1H, Ar), 7.87 (d, J = 7.6 Hz, 1H, Ar), 8.65 (m, 2H, Ar); MS (ES+) m/z = 393 (MH^+). Anal. ($C_{23}H_{24}N_2O_4$) C, H, N.

(2*R,3*S**)-1-(Phenanthren-2-ylmethyl)piperazine-2,3-dicarboxylic Acid (23).** (2*R**,3*S**)-1-Phenanthren-2-ylmethylpiperazine-2,3-dicarboxylic acid dimethyl ester (**22**) (0.40 g, 1.0 mmol) was stirred for 24 h at room temperature in tetrahydrofuran/water (60 mL, 2:1) with excess lithium hydroxide (0.42 g, 10.0 mmol). The solution was then acidified to pH 3 with 2 M HCl (aq), evaporated to half volume under reduced pressure, diluted with water (30 mL), and again evaporated to half volume under reduced pressure. The solid was collected by filtration, washed with water and diethyl ether, and allowed to air-dry, giving **23** (320 mg, 81%) as a white solid: mp 190−193 °C (dec); ^{1}H NMR (270 MHz, D_2O/NaOD, pH 11) δ 2.32−2.66 (m, 2H, HNCH_2), 2.89−3.06 (m, 2H, HNCH_2CH_2), 3.49 (d, J = 4.0 Hz, 1H, NCHCO_2H), 3.63 (d, $J_{A,B}$ = 12.9 Hz, 1H, NCH_2Ar), 3.71 (d, J = 4.0 Hz, 1H, NCHCO_2H), 3.99 (d, $J_{B,A}$ = 12.9 Hz, 1H, NCH_2Ar), 7.53−7.71 (m, 5H, Ar), 7.76−7.90 (m, 2H, Ar), 8.45−8.61 (m, 2H, Ar); MS (ES+) m/z = 391.2 (M + H), 413.1 (M + H + Na). Anal. ($C_{21}H_{20}N_2O_4 \cdot 1.5H_2O$) C, H, N.

NR Subunit Expression in *Xenopus* oocytes. cDNA encoding the NMDAR1a subunit was a generous gift of Dr Shigetada Nakanishi (Kyoto, Japan). cDNAs encoding NR2A, NR2C, and NR2D were kindly provided by Dr. Peter Seeburg (Heidelburg, Germany) and the NR2B [5′UTR]-cDNA was a generous gift of Drs. Dolan Pritchett and David Lynch (Philadelphia, PA). Plasmids were linearized with *Not*I (NR1a), *Eco*RI (NR2A, NR2C and NR2D), or *Sal*I (NR2B), and transcribed in vitro with T3 (NR2A, NR2C), SP6 (NR2B), or T7 (NR1a, NR2D) RNA polymerase using the mMessage mMachine Transcription Kits (Ambion, Austin, TX).

Oocytes were removed from mature female *Xenopus laevis* (Xenopus One, Ann Arbor, MI) as previously described.[8] NMDA receptor subunit RNAs were dissolved in sterile distilled H_2O. NR1a and NR2 RNAs were mixed in a molar ratio of 1:3. In all, 50 nL of the final RNA mixture was microinjected (15−30 ng total) into the oocyte cytoplasm. Oocytes were incubated in ND-96 solution at 17 °C prior to electrophysiological assay (1−5 days).

Electrophysiological Characterization of Recombinant NMDA Receptors. Electrophysiological responses were measured using a standard two-microelectrode voltage clamp as previously described.[8] The voltage clamp used was a Warner Instruments (Hamden, CT) model OC-725B Oocyte Clamp, designed to provide fast clamp of large cells. The recording buffer contained 116 mM NaCl, 2 mM KCl, 2 mM $BaCl_2$, and 5 mM HEPES, pH 7.4. Response magnitude was determined by the steady plateau response elicited by bath application of 10 μM l-glutamate plus 10 μM glycine at a holding potential of 60 mV. Five oocytes were tested against 100 μM NMDA/10 μM glycine-evoked responses. Response amplitudes for the four heteromers were generally between 30 and 100 nA. Attempts were made to keep response magnitudes within this range to minimize activation of the endogenous Cl^- current. The presence of a plateau response was taken as an indication of the lack of significant activation of the endogenous Cl^- current by Ba^{2+} in these cells. Antagonist inhibition curves were fit (GraphPad Prism, ISI Software, San Diego, CA) according to the equation $I = I_{max} - I_{max}/[1 + (IC_{50}/A)^n]$, where I_{max} is the current response in the absence of antagonist, A is the antagonist concentration, and IC_{50} is the antagonist concentration producing half-maximal inhibition. Apparent K_i values were determined by correcting for agonist affinity according to the equation $IC_{50} = IC_{50}(obs)/1 + ([agonist]/EC_{50})$ as described.[33]

Electrophysiological Characterization of 16e on Neonatal Rat Motoneurones. All experiments were carried out in 1−4-day-old Wistar rats of either sex as described previously.[12] To examine the effects of **16e** on direct depolarizations of motoneurones induced by NMDA (50 μM), experiments were conducted in standard medium containing TTX (10 μM for 2 min then 0.1 μM continuously). NMDA was applied for 1 min and the degree of depolarization of the motoneurone was measured by peak amplitude. The ability of **16e** to selectively reduce the peak amplitude of the NMDA-induced responses was then measured. NMDA-induced responses recovered after a 30 min washout of the antagonist. To calculate the pA_2 value for the antagonism of NMDA-induced depolarizations by **16e**, noncumulative concentration−response curves were constructed both in the absence and presence of 0.5, 0.7, 1, 2, and 3 μM **16e** and dose ratios (DR) estimated from the equation DR = EC_{50} of NMDA in the presence of **16e**/EC_{50} of NMDA in the absence of **16e**. A graph (Schild plot) of log(DR − 1) vs log [PPDA] M was then plotted using GraphPad Prism version 2.0.

Acknowledgment. We thank Drs Shigetada Nakanishi, David Lynch, and Peter Seeburg, for providing NMDA receptor cDNA constructs, and Dr Yves Auberson at Novartis Pharma AG, Basel, Switzerland, for providing PEAQX. This work was supported by NIH Grant MH60252.

Supporting Information Available: Six tables containing the X-ray crystallographic crystal data of derivative **10**. This material is available free of charge via the Internet at http://pubs.acs.org.

References

(1) Dingledine, R.; Borges, K.; Bowie, D.; Traynelis, S. F. The glutamate receptor ion channels. *Pharmacol. Rev.* **1999**, *51*, 7−61.

(2) Jane, D. E.; Tse, H.-W.; Skifter, D. A.; Christie, J. M.; Monaghan, D. T. Glutamate receptor ion channels: Activators and inhibitors. In *Pharmacology of Ionic Channel Function: Activators and Inhibitors;* Endo, M., Kurachi Y., Mishina, M., Eds.; Springer-Verlag: Berlin, 2000; pp 415−459.
(3) Choi, D. Antagonizing excitotoxicity: A therapeutic strategy for stroke? *Mt. Sinai J. Med.* **1998**, *65*, 133−138.
(4) Das, S.; Sasaki, Y. F.; Rothe, T.; Premkumar, L. S.; Takasu, M.; Crandall, J. E.; Dikkes, P.; Conner, D. A.; Rayudu, P. V.; Cheung, W.; Vincent Chen, H.-S.; Lipton, S. A.; Nakanishi, N. Increased NMDA current and spine density in mice lacking the NMDA receptor subunit NR3A. *Nature (London)* **1998**, *393*, 377−381.
(5) Laube, B.; Hirai, H.; Sturgess, M.; Betz, H.; Kuhse, J. Molecular determinants of agonist discrimination by NMDA receptor subunits: Analysis of the glutamate binding site on the NR2B subunit. *Neuron* **1997**, *18*, 493−503.
(6) Hirai, H.; Kirsch, J.; Laube, B.; Betz, H.; Kuhse, J. The glycine binding site of the *N*-methyl-D-aspartate receptor subunit NR1: Identification of novel determinants of co-agonist potentiation in the extracellular M3-M4 loop region, *Proc. Natl. Acad. Sci. U.S.A.* **1996**, *93*, 6031−6036.
(7) Ishii, T.; Moriyoshi, K.; Sugihara, H.; Sakurada, K.; Kadotani, H.; Yokoi, M.; Akazawa, C.; Shigemoto, R.; Mizuno, N.; Masu, M.; Nakanishi, S. Molecular characterization of the family of the *N*-methyl-D-aspartate receptor subunits. *J. Biol. Chem.* **1993**, *268*, 2836−2843.
(8) Buller, A. L.; Larson, H. C.; Schneider, B. E.; Beaton, J. A.; Morrisett R. A.; Monaghan, D. T. The molecular basis of NMDA receptor subtypes: Native receptor diversity is predicted by subunit composition. *J. Neurosci.* **1994**, *14*, 5471−5484.
(9) Buller, A. L.; Monaghan, D. T. Pharmacological heterogeneity of NMDA receptors: Characterization of NR1a/NR2D heteromers expressed in *Xenopus* oocytes. *Eur. J. Pharmacol*. **1997**, *320*, 87−94.
(10) Monaghan, D. T.; Andaloro, V. J.; Skifter, D. A. Molecular determinants of NMDA receptor pharmacological diversity. *Prog. Brain Res.* **1998**, *116*, 158−177.
(11) Christie, J. M.; Jane, D. E.; Monaghan, D. T. Native *N*-methyl-D-aspartate receptors containing NR2A and NR2B subunits have pharmacologically distinct competitive antagonist binding sites. *J. Pharmacol. Exp. Ther.* **2000**, *292*, 1169−1174.
(12) Evans, R. H.; Francis, A. A.; Jones, A. W.; Smith, D. A. S.; Watkins, J. C. The effects of a series of ω-phosphonic α-carboxylic amino acids on electrically evoked and amino acid induced responses in isolated spinal cord preparations. *Br. J. Pharmacol*. **1982**, *75*, 65−75.
(13) Davies, J.; Evans, R. H.; Herrling, P. L.; Jones, A. W.; Olverman, H. J.; Pook, P.; Watkins, J. C. CPP a new and selective NMDA antagonist. Depression of central neuron responses, affinity for [^{3}H]D-AP5 binding sites on brain membranes and anticonvulsant activity. *Brain Res.* **1986**, *382*, 169−173.
(14) Ikeda, K.; Nagasawa, M.; Mori, H.; Araki, K.; Sakimura, K.; Watanabe, M.; Inoue, Y.; Mishina, M. Cloning and expression of the epsilon 4 subunit of the NMDA receptor channel. *FEBS Lett*. **1992**, *313*, 34−38.
(15) Laurie, D. J.; Seeburg, P. H. Ligand affinities at recombinant *N*-methyl-D-aspartate receptors depend on subunit composition. *Eur. J. Pharmacol.* **1994**, *268*, 335−345.
(16) Auberson, Y. P.; Allgeier, H.; Bischoff, S.; Lingenhoehl, K.; Moretti, R.; Schmutz, M. 5-Phosphonomethylquinoxalinediones as competitive NMDA receptor antagonists with a preference for the human 1A/2A, rather than 1A/2B receptor composition. *Bioorg. Med. Chem. Lett.* **2002**, *12*, 1099−1102.
(17) Feng, B.; Tse, H. W.; Skifter, D. A.; Morley, R.; Jane, D. E.; Monaghan, D. T. NMDA receptor subtype selectivity of (2*R**,3*R**)-1-(biphenyl-4-carbonyl)piperazine-2,3-dicarboxylic acid derivatives. *Br. J. Pharmacol.* **2004**, *141*, 508−516.
(18) Felder, E.; Maffei, S.; Pietra, S.; Pitrè, D. Über die katalytische hydrierung von pyrazinecarbonsäuren. *Helv. Chim. Acta* **1960**, *43*, 888−896.
(19) Yashunskii, V. G.; Samoilova, O. I.; Shchukina, M. N. Complex forming substances. VI. Synthesis of cyclic analogues of cyanotriacetic and ethylenediaminetetraacetic Acids. *J. Gen. Chem. USSR* **1961**, *31*, 2158−2162.
(20) Schneider, H. J. Equilibria between diastereomeric substituted 1,2-dibromoethanes. *Justus Liebigs Ann. Chem.* **1972**, *761*, 150−161.
(21) Guthrie, J. P.; O'Leary, S. General base catalysis of β-elimination by a steroidal enzyme model. *Can. J. Chem.* **1975**, *53*, 2150−2156.
(22) Huisgen, R.; Scheer, W.; Szeimies G.; Huber, H. 1.3-Cycloadditions von azomethin-yliden aus aziridin-carbonestern. *Tetrahedron Lett.* **1966**, *7*, 397−404.
(23) Jane, D. E.; Olverman, H. J.; Watkins, J. C. Agonists and competitive antagonists: Structure−activity and molecular modelling studies. In *The NMDA receptor*; Collingridge G. L.; Watkins J. C., Eds.; Oxford University Press: Oxford, UK, 1994; pp 31−104.
(24) Jane, D. E. Antagonists acting at the NMDA receptor complex: Potential for therapeutic applications. In *Glutamate and GABA receptors and transporters;* Krogsgaard-Larsen, P., Egebjerg, J., Schousboe, A., Eds.; Taylor and Francis: London, 2002; pp 69−98.
(25) Bigge, C. F. Structural requirements for the development of potent *N*-methyl-D-aspartic acid (NMDA) receptor antagonists. *Biochem. Pharmacol.* **1993**, *45*, 1547−1561.
(26) Cheung, N. S.; O'Callaghan, D.; Ryan, M. C.; Dutton, R.; Wong, M. G.; Beart, P. M. Structure−activity relationships of competitive NMDA receptor antagonists. *Eur. J. Pharmacol.* **1996**, *313*, 159−162.
(27) Davies, J.; Jones, A. W.; Sheardown, M. J.; Smith, D. A. S.; Watkins, J. C. Phosphono dipeptides and piperazine derivatives as antagonists of amino acid-induced and synaptic excitation in mammalian and amphibian spinal cord. *Neurosci. Lett*. **1984**, *52*, 79−84.
(28) Ganong, A. H.; Jones, A. W.; Watkins, J. C.; Cotman, C. W. Parallel antagonism of synaptic transmission and kainate/quisqualate responses in the hippocampus by piperazine-2,3-dicarboxylic acid analogues. *J. Neurosci*. **1986**, *6*, 930−937.
(29) Armstrong, N.; Sun, Y.; Chen, G. Q.; Gouaux, E. Structure of a glutamate-receptor ligand-binding core in complex with kainate. *Nature* **1998**, *395*, 913−917.
(30) Furukawa, H.; Gouaux, E. Mechanisms of activation, inhibition and specificity: Crystal structures of the NMDA receptor NR1 ligand-binding core. *EMBO J* **2003**, *22*, 2873−2885.
(31) Hrabetova, S.; Serrano, P.; Blace, N.; Tse, H. W.; Skifter, D. A.; Jane, D. E.; Monaghan, D. T.; Sacktor, T. C. Distinct NMDA receptor subpopulations contribute to long-term potentiation and long-term depression induction. *J. Neurosci. (Online)* **2000**, *20*, RC81.
(32) Lozovaya, N. A.; Grebenyuk, S. E.; Tsintsadze, T. S.; Feng, B.; Monaghan, D. T.; Krishtal, O. A. Extrasynaptic NR2B and NR2D subunits of NMDA receptors shape 'superslow' afterburst EPSC in rat hippocampus. *J Physiol. (London)* **2004**, *558*, 451−463.
(33) Durand, G. M.; Gregor, P.; Zheng, X.; Bennett, M. V.; Uhl, G. R.; Zukin, R. S. Cloning of an apparent splice variant of the rat *N*-methyl-D-aspartate receptor NMDAR1 with altered sensitivity to polyamines and activators of protein kinase C. *Proc. Natl. Acad. Sci. U.S.A.* **1992**, *89*, 9359−9363.

JM0492498